Development and Validation of a Kinematically Accurate Upper-Limb Exoskeleton Digital Twin for Stroke Rehabilitation

Ratschat, Alexandre; Lomba, Tiago M. C.; Gasperina, Stefano D.; Marchal-Crespo, Laura

DOI
10.1109/ICORR58425.2023.10304719

Publication date
2023

Document Version
Final published version

Published in
Proceedings of the 2023 International Conference on Rehabilitation Robotics (ICORR)

Development and Validation of a Kinematically Accurate Upper-Limb Exoskeleton Digital Twin for Stroke Rehabilitation

Alexandre Ratschat[1,2], Tiago M. C. Lomba[1], Stefano Dalla Gasperina[1] and Laura Marchal-Crespo[1,2]

***Abstract*— Rehabilitation robotics combined with virtual reality using head-mounted displays enable naturalistic, immersive, and motivating therapy for people after stroke. There is growing interest in employing digital twins in robotic neurorehabilitation, e.g., in telerehabilitation for virtual coaching and monitoring, as well as in immersive virtual reality applications. However, the kinematic matching of the robot's visualization with the real robot movements is hardly validated, potentially affecting the users' experience while immersed in the virtual environment due to a visual-proprioceptive mismatch. The kinematic mismatch may also limit the validity of assessment measures recorded with the digital twin. We present the development and low-cost kinematic validation of a digital twin of a seven active degrees-of-freedom exoskeleton for stroke rehabilitation. We validated the kinematic accuracy of the digital twin end-effector by performing two tasks—a planar reaching task and a 3D functional task—performed by a single healthy participant. We computed the end-effector position and rotation from the forward kinematics of the robot, the digital twin, and data recorded from the real robot using a low-cost tracking system based on HTC VIVE trackers and compared them pair-wise. We found that the digital twin closely matches the forward kinematics and tracked movement of the real robot and thus provides a reliable platform for future research on digital twins for stroke rehabilitation.**

I. Introduction

Rehabilitation robotics can be ubiquitously found in clinical settings to support therapists in providing intensive and frequent training to enhance the recovery of people after stroke [1], [2]. Robotic training devices are often combined with virtual reality (VR) applications displayed on a 2D screen to allow users to play motivating serious games or practice simulated activities of daily living [3]. Recent research has incorporated more immersive VR (IVR) using off-the-shelf head-mounted displays (HMDs) that provide virtual training environments from a first-person perspective together with an avatar animated following the actual movements of the users. These IVR applications have been shown to enhance movement quality [4], motivation, and embodiment [5], compared to conventional computer screens. However, it is still an open question how and if rehabilitation robots should be visualized in the virtual environment (VE) and how this visualization might influence the users' affects [6].

In state-of-the-art systems that combine rehabilitation robotics with IVR, the robot is rarely visualized in the VE. There are currently only a few examples of rehabilitation robot digital twins—digital replicas of real-life physical systems—in the field, mainly in telerehabilitation applications. These digital twins are usually displayed on 2D screens to facilitate the monitoring and control of rehabilitation robots by therapists located remotely [7], [8]. For example, Modi et al. developed a digital twin of a five-degrees-of-freedom (5-DOF) robotic manipulator as part of an experimental telerehabilitation framework [7]. They showed that the digital twin enabled the experimenter to monitor and alter pre-determined exercises from a separate room while a mock patient performed the exercises with the real robot. However, they did not provide any indication about the kinematic accuracy of the digital twin compared to the real robot.

Digital twins have barely been employed to investigate the effect of visualizing the rehabilitation robot "worn" by the user on factors such as users' motivation, embodiment, or presence, all factors related to better motor learning [9]. In a recent study with healthy participants, Wenk et al. evaluated how the potential visuo-haptic sensory conflict between what users see and feel during robotic training might hamper the users' affects [6]. They found that the visualization of the digital twin of an end-effector upper-limb rehabilitation robot during a motor task in IVR did not impact healthy participants' motivation, embodiment, presence, and task performance compared to not visualizing the robot. Yet, visualizing the robot resulted in a greater subjective report of participants' effort. While these studies provided some first insights into the use of digital twins in robotic rehabilitation applications, there are still many open questions regarding how to exploit their use to enhance the effectiveness of VR-based neurorehabilitation.

However, before investigating the use of digital twins in rehabilitation, it is crucial to first evaluate how reliable those visualizations are in accurately replicating the kinematics of their real counterparts. Some challenges have been encountered when animating avatars using the forward kinematics of exoskeletons. For instance, Wenk et al. noticed that the end-effector position obtained from the position sensors and forward kinematics calculations of a commercial rehabilitation exoskeleton had a visible offset from the actual end-effector position [4]. These mismatches could arise from offsets at each joint due to inadequate calibrations, sensor in-

*This work was funded by the Dutch Research Council (NWO, VIDI Grant Nr. 18934)

[1]Alexandre L. Ratschat, Tiago M. C. Lomba, Stefano Dalla Gasperina, and Laura Marchal-Crespo are with the Motor Learning and Neurorehabilitation Laboratory, Department of Cognitive Robotics, Delft University of Technology, Delft, The Netherlands.

[2]Alexandre L. Ratschat and Laura Marchal-Crespo are with the Department of Rehabilitation Medicine, Erasmus MC, Rotterdam, The Netherlands a.l.ratschat@tudelft.nl

accuracies, or misused technology by non-technical oriented users. While small visual offsets do not seem to harm task performance [10], they might hamper the users' experience [11]. Importantly, using inaccurate robot visualizations and forward kinematic models to calculate clinically-relevant kinematic outcome measures may be misleading since their validity is not guaranteed. To solve the mismatch between the real robot and digital twin, Wenk et al. attached three HTC VIVE trackers to track several links of the mechanical structure and used this information to animate their human avatars. Yet, they did not thoroughly validate the kinematic accuracy of the modeled avatar arm, nor did they include a visualization of the upper-limb exoskeleton.

This work presents the development and low-cost kinematic validation of a 7-DOF upper-limb exoskeleton digital twin. We compared the end-effector movement and two clinically-relevant outcome measures, namely peak speed and movement smoothness, between the digital twin, the robot's forward kinematics, and the tracked real robot movements using a relatively low-cost solution based on four HTC VIVE trackers (VIVE Trackers 3.0, HTC Corporation, Taiwan). By developing and validating the visualization of the exoskeleton, we are providing a reliable platform for future developments in telerehabilitation and potential investigations on the effect of digital twin visualizations on patients' affects—e.g., motivation, embodiment, and agency—in a controllable virtual environment. This may bring new rehabilitation opportunities, ultimately enhancing the users' recovery and quality of life.

II. Methods

A. Digital Twin Implementation

A modified version of the upper-limb rehabilitation exoskeleton ARMin [12], [13] was used as the basis for the development of the digital twin. The ARMIN features six active DOFs and three passive DOFs; the latter adapt the exoskeleton to different arm sizes. The exoskeleton was extended with the hand module PRIDE developed by Rätz et al. [14], enabling full finger flexion and extension and leading to overall seven active DOFs (Fig. 1a).

The digital twin of the exoskeleton (Fig. 1b) was implemented starting from the CAD model of the robot. Each link of the exoskeleton was separately imported into the three-dimensional (3D) computer graphics software Blender (Blender version 3.2.2, Blender Organization, Netherlands). The origin frame of each link was defined to be aligned with the origin of each rotational and translational joint. This ensured that in the next steps, each link would move in the same manner as the links of the real robot. Following, each link was imported into the Unity game engine (Unity Editor 2021.3.2f, Unity Technologies, USA), starting from the robot's base and ending with the hand module. The base of the ARMin (see Fig. 1a) was rigidly placed on the floor of the virtual environment (VE). Each link of the exoskeleton was placed manually as precisely as possible from the more proximal to the most distal links of the robotic serial chain. Each link was included as a *child* of the previous link in

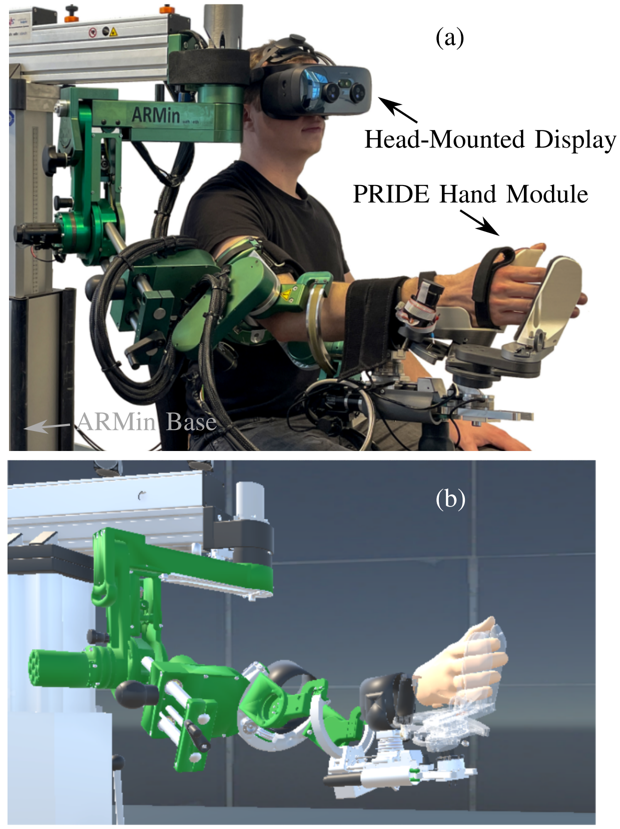

Fig. 1: Experimental setup: (a) A user wearing a head-mounted display (Varjo XR-3, Varjo, Finland). The ARMin upper-limb exoskeleton was combined with the PRIDE hand module [14]. (b) The digital twin implemented in Unity.

Unity. Thus, the link follows the movement of the *parent*, i.e., the previously collocated link. All links were included as kinematic objects, and thus, the physics engine of Unity was disabled since the real robot provided the joint positions. Also, the DOFs and range of motions (ROMs) of each virtual link were limited according to the DOFs and ROMs of the real robot links.

Once the digital twin is created, aligning it with the real-world robot is critical to provide the user with a seamless and coherent experience between the physical and virtual environments and, thus, prevent visual-proprioceptive incongruities that might hamper the users' sense of presence and embodiment. While alignment can be achieved using different methods, such as sensor fusion techniques or motion capture systems, we opted for a low-cost off-the-shelf solution consisting of four HTC VIVE trackers 3.0 (HTC Corporation, Taiwan) based on infrared optical tracking technology and an inertial measurement unit (IMU), and three SteamVR Base Stations 2.0 (HTC Corporation, Taiwan). The total cost of the system was below 1500 €.

As shown in Fig. 2, trackers A and B were placed on the top of the boom, aligned with the x-axis of the robot coordinate frame $\{O\}$. Here, tracker A coincided with the origin of the robot coordinate frame $\{O\}$. The tracker C was placed on the column of the robot and thus on the xz-plane of the robot coordinate frame. Additionally, tracker D was placed close to the robot's end-effector to track its position and rotation. During the VE initialization, the positions of trackers A–C are averaged for three seconds and following, the origin of the digital twin, which is located at the same point as the position of tracker A on the real robot, is moved to coincide with the averaged position of tracker A. Furthermore, the digital twin is rotated to align with the axes defined by the averaged positions of trackers A–C.

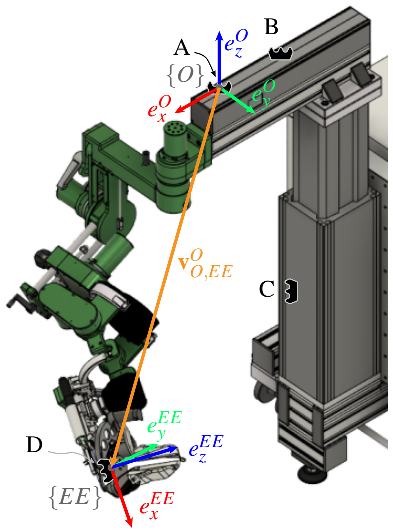

Fig. 2: Trackers placement and end-effector pose definition. Trackers A and B were placed on the boom of the ARMin, in line with the x-axis of the real robot frame $\{O\}$ and A (center of the tracker) coinciding with the frame origin. Tracker C was placed on the centerline of the vertical column, spanning the xz-plane with trackers A and B. Tracker D was placed under the hand module on the end-effector. The pose of the end-effector is defined by the translation $\mathbf{v}_{O,EE}^O$ and the rotation $\mathbf{R}_{O,EE}$ between frames $\{O\}$ and $\{EE\}$.

The communication between the digital twin and the exoskeleton occurred over a network connection using the User Data Protocol (UDP). The exoskeleton continuously sent the joint angles, the end-effector position and rotation calculated by the forward kinematics, and the passive joint positions to the digital twin at a frequency of 250 Hz. The digital twin continuously adjusted the rotation of its individual joints to mirror the received movement of the real robot joints at a frequency of approximately 70–80 Hz.

B. *Kinematic Evaluation of the Digital Twin*

The kinematic evaluation of the digital twin was performed with a single participant (30 y.o., male) wearing the exoskeleton on the right arm. The participant visualized the VE and the digital twin from the first-person perspective through an HMD (Varjo XR-3, Varjo, Finland). The robot was controlled using a highly transparent disturbance observer [15].

1) Evaluation Tasks: The participant performed two tasks based on the consensus-based core recommendations from the second Stroke Recovery and Rehabilitation Roundtable (SRRR) [16]. The SRRR recommends two tasks for patients' kinematic measures: a *planar reaching task* and a *3D functional task*. The planar reaching task chosen for our evaluation consisted of reaching toward six targets equally distributed on a circle of 15 cm radius together with an additional target placed at the center of the circle (Fig. 3a). Starting from the center position, the participant moved the end-effector to a target, stopped for 1–2 s, and returned to the center. This movement was repeated for all targets.

The selected 3D functional task mimics an activity of daily living: drinking from a cup. The task involved moving the robot end-effector from a starting position, indicated by a disk, to a virtual cup represented by a cylinder in the VE, then to the mouth before returning to the cylinder, and finally back to the starting position (Fig. 3b). For simplicity, grasping the cup was not required; touching the cylinder with the virtual hand was sufficient. Both tasks were performed at a self-paced slow, medium, and fast speed to assess the kinematic accuracy and outcome measures for a more comprehensive application range. For each speed condition, the planar reaching task was performed once, and the 3D functional task was performed three times. For the analysis of the 3D functional task, the data of the three repetitions are combined and not regarded separately.

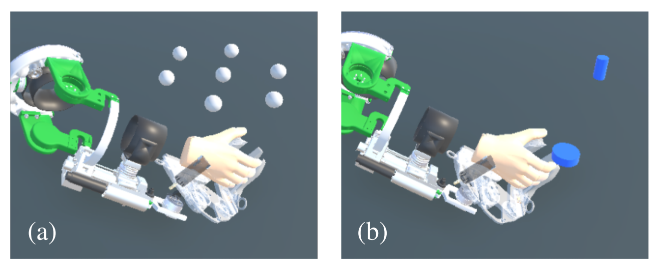

Fig. 3: The VEs of the tasks performed to evaluate the digital twin kinematic accuracy: (a) planar reaching task with six targets equally spaced in a circle around a center point and (b) 3D functional hand-to-mouth task with a disk denoting the starting position and a cylinder representing a cup. Note that participants saw the VE from a first-person perspective.

2) End-Effector Pose Accuracy: We assessed the kinematic accuracy of the end-effector pose (position and rotation) of the digital twin (**DT**)—measured directly in the VE and referenced to the origin of the robot coordinate frame—by comparing it to the pose calculated through the forward kinematics (**FK**) of the robot control in the real-world reference frame—based on the measured joint angles of the robot—and to the pose of tracker D placed on the real robot end-effector (**RR**)—without relying on the measured robot joint positions. To compare the measurements from the different methods, they were transformed to be within the real robot frame $\{O\}$. Two metrics were calculated to compare the end-effector pose between measurement methods: 1) the absolute position difference and 2) the absolute rotation difference between the end-effector poses, representing the translational and rotational differences, respectively.

3) Clinically Relevant Kinematic Outcome Measures: We calculated two clinically relevant kinematic outcome measures usually employed for assessing patients' movement quality—namely, peak speed and movement smoothness—using the three end-effector pose calculation methods and compared the outcome measures between them. The speed of the end-effector was obtained by dividing the norm of the position difference between two consecutive time steps by their time difference. Outliers in the speed data were detected using the Interquartile Range (IQR) method, defined as the distance between the first quartile ($Q1$) and the third quartile ($Q3$) of the dataset. Data points below $Q1 - 1.5IQR$ or above $Q3 + 1.5IQR$ were replaced by a linear interpolation of their neighboring points. The percentage of outliers per measurement method was: 0.63 % (FK), 0.61 % (DT), and 1.76 % (RR). The speed data was then re-sampled to a frequency of 70 Hz using the *interp1d* function of Scipy (Version 1.10.1). The speed time series were then filtered with a first-order low-pass Butterworth filter at a cutoff frequency of 20 Hz since 98% of human activity is below 10 Hz [17]. The movement smoothness was calculated using the SPectral ARC length (SPARC) [18], where a low absolute SPARC value indicates high movement smoothness. To calculate the SPARC, the maximum cut-off frequency was set to $\omega_c^{max} = 20\,\text{Hz}$, and we evaluated three values for the amplitude threshold $\overline{V} = \{0.01, 0.025, 0.05\}$, which is a (unitless) threshold on the normalized magnitude spectrum. Higher values of $\overline{V}$ result in lower cut-off frequencies and higher noise robustness but lower SPARC sensitivity. All data processing was done in Python 3.8.10 (Python Software Foundation, USA).

III. Results

Fig. 4 shows the end-effector positions calculated using the three methods (FK: Forward kinematics; DT: digital twin; RR: tracker on the real robot) for both evaluation tasks performed at medium speed.

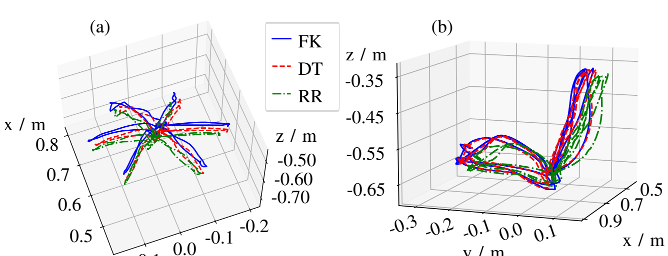

Fig. 4: End-effector positions recorded at medium speed for the three pose calculation methods and two tasks: (a) planar reaching task and (b) 3D functional (drinking) task.

The planar reaching task was performed at a mean speed of 0.06, 0.08, and 0.1 m/s and the 3D functional task at 0.13, 0.17, and 0.28 m/s for the slow, medium and fast speeds, respectively. The mean speed of the planar reaching task includes the 1–2 s of rest at each target, yielding a slower overall mean speed. We noted that the speed data of the trackers (RR) was noisy compared to the other two speed calculations (Fig. 5), even though it was filtered.

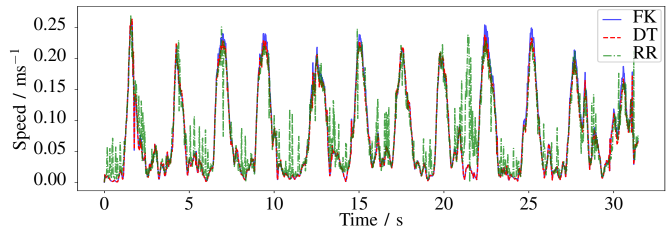

Fig. 5: Filtered speed profile for the three measurement methods of the planar reaching task at medium speed.

A. End-Effector Pose Accuracy

The pairwise absolute mean differences in position and orientation of the end-effector between the three measurement methods, i.e., FK–DT, FK–RR, and DT–RR, for the two evaluation tasks and at different movement speeds are shown in Table I. Notably, there was a positional offset between methods distributed along the x, y, and z-axis (see Fig. 4(a)). The positional and rotational mean absolute differences were the lowest between the FK and DT methods, while the absolute rotational differences were relatively high for the FK–RR and DT–RR comparisons.

Fig. 6 illustrates the pairwise end-effector pose discrepancies during the two evaluation tasks. The difference between the forward kinematics (FK) and the digital twin (DT) methods, depicted as a solid blue line, consistently showed the smallest absolute position and rotation differences. Note that the pair-wise absolute differences followed a periodic behavior as a result of the repetitive tasks.

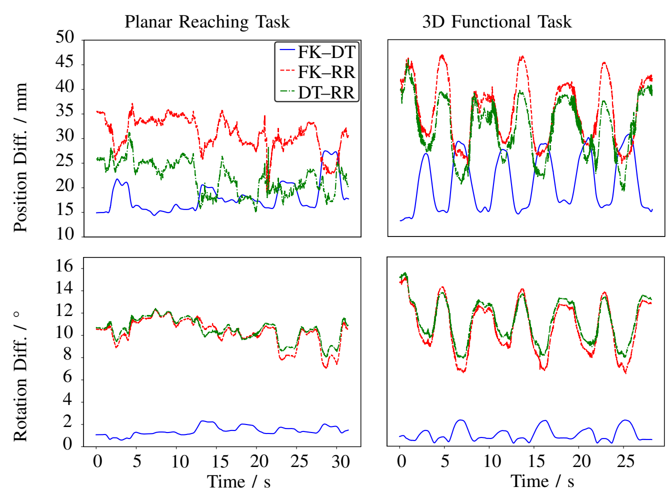

Fig. 6: Pair-wise absolute differences in end-effector position (upper row) and rotation (lower row) between the three calculation methods during the planar reaching and 3D functional tasks.

B. Peak Speed and Movement Smoothness

Fig. 7 displays the peak speed and movement smoothness for both tasks. It can be noticed that the computed peak

TABLE I: Mean and standard deviation (SD) of the end-effector position and rotation absolute differences between measurement methods: forward kinematics (FK), digital twin (DT), and trackers on the real robot (RR).

Task	Abs. Position Difference: Mean (SD) / mm			Abs. Rotation Difference: Mean (SD) / °		
	FK–DT	FK–RR	DT–RR	FK–DT	FK–RR	DT–RR
Planar Reaching (Slow)	18.1 (2.85)	31.4 (3.33)	22.0 (3.44)	1.41 (0.315)	10.20 (0.894)	10.47 (0.726)
Planar Reaching (Medium)	18.1 (3.15)	31.0 (3.28)	22.1 (3.28)	1.42 (0.394)	10.25 (1.185)	10.52 (0.968)
Planar Reaching (Fast)	19.9 (2.47)	27.6 (3.02)	18.4 (3.46)	1.83 (0.212)	8.10 (1.096)	8.56 (0.847)
3D Functional (Slow)	20.8 (5.12)	34.8 (5.66)	30.1 (5.97)	1.02 (0.535)	10.55 (2.003)	11.03 (1.713)
3D Functional (Medium)	21.1 (5.49)	35.6 (6.35)	32.2 (6.02)	1.07 (0.578)	10.72 (2.277)	11.29 (1.885)
3D Functional (Fast)	22.3 (5.08)	34.9 (5.13)	31.2 (4.95)	1.36 (0.678)	9.64 (2.442)	10.50 (1.922)

speeds were closely aligned across all tasks and methods. Notably, in the planar reaching task, the smoothness decreased with increasing speed. Conversely, in the 3D functional task, higher speeds led to smoother movements. Lower values of $\overline{V}$ led to reduced smoothness when using the FK and DT methods. However, the overall trend remained consistent. Regarding the RR method, for $\overline{V} = 0.05$, the smoothness was similar to the other two methods. Nonetheless, smoothness drastically decreased for lower $\overline{V}$, altering the observed trend.

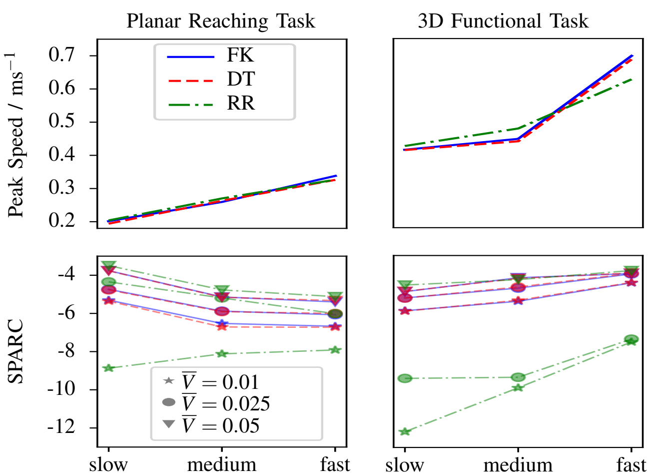

Fig. 7: Peak speed and movement smoothness calculated from each end-effector pose calculation method, at each speed condition, and for each evaluation task.

IV. Discussion

We presented the creation of an upper-limb exoskeleton digital twin with seven active and three passive degrees of freedom. Furthermore, we proposed a low-cost kinematic validation method based on off-the-shelf HTC VIVE trackers to compare the kinematic accuracy of three different end-effector pose calculations, namely the forward kinematics of the robot, the digital twin, and trackers attached to the real robot.

A. End-Effector Pose Accuracy

We found that the end-effector poses measured directly from the digital twin are close (less than 32.2 mm mean absolute difference in position and 11.29 ° mean absolute difference in orientation) to those calculated from the forward kinematics of the robot and the trackers placed on the real robot. Comparing the FK and RR methods yielded similar results—the dynamic spatial accuracy found had the same order of magnitude as the mean errors in translation tracking accuracy of 11.1 mm found by Kuhlmann et al. for the same trackers with two base stations [19]. They measured the spatial dynamic accuracy of the trackers by attaching a VIVE tracker (3.0) to a highly accurate robotic arm and performing a conical spiral movement at 50 mm/s. Possible factors contributing to the observed minor differences in position and rotation include minor discrepancies in the robot coordinate frame identification, slight variations in the joint alignment of the digital twin, small calibration errors of the real robot joint offset, and inaccuracies in the placement of the trackers. Notably, the larger rotation differences between the FK/DT measurement methods and the RR method are likely due to a constant rotational offset of the tracker on the robot's end-effector. This is supported by the lower rotation differences between the DT and FK, which do not rely on the end-effector tracker.

Whether these observed differences might influence task performance and users' experience is still an open question. However, Groen and Werkhoven found no impact on task performance while manipulating blocks with a lateral offset error of 10 cm [10]. Thus, we argue that the small position errors in the visualization of our digital twin may not affect the users' task performance while training with the digital twin in IVR.

B. Clinically-Relevant Outcome Measures

The SRRR recommends recording kinematic measures as supporting clinically-relevant outcome measures using high-quality optical tracking systems [16]. We found that with our low-cost kinematic validation method, the peak speed and movement smoothness at the end-effector can be computed directly from the forward kinematics and the digital twin, with similar results to those calculated from the HTC VIVE trackers on the real robot. The impact of varying the amplitude threshold on the SPARC smoothness measures can differ depending on the signal characteristics. Notably, when comparing values obtained from the digital encoders with those calculated from tracker data, we observed that the former exhibited higher robustness to changes in the amplitude threshold.

C. Limitations and Future Work

There are some limitations to our work. First, the low-cost HTC VIVE tracking system resulted in noisy position data, with occasional position drift, jitter, and connection losses, similar to the issues reported by Niehorster et al. [20]. This affected the kinematic data of the real robot tracking measurement method, limiting the robustness of the end-effector pose comparison and the calculation of the kinematic outcome measures. While this limitation can be addressed using higher-quality motion capture camera-based systems, the relatively small differences observed between the RR, FK, and DT calculations suggest that the HTC VIVE trackers enable kinematic validations with acceptable precision and easy setup without substantial financial costs.

A second limitation is that we recorded a relatively small amount of data from only two tasks and one participant. This limits the robustness and generalization of our results. Future research should include an experiment with an appropriate number of participants from a diverse population, and several tasks that cover a larger joint-based workspace should be repeated at least 15 times, as recommended by Kwakkel et al. [16].

Now that the kinematic accuracy of our virtual twin has been shown, future work includes the visualization of the user through avatars animated using the digital twin kinematics and the investigation of how the observed mismatch between the digital twin and the forward kinematics might impact the user experience. Furthermore, we plan to evaluate how the appearance of the digital twin—namely, its color, texture, and material—influences the users' affects, such as motivation and agency during the training of motor tasks.

V. Conclusion

We presented the creation of a digital twin in Unity for an augmented 7-DOF ARMin exoskeleton. Furthermore, we demonstrated a method to validate the kinematic accuracy of the digital twin using relatively low-cost HTC VIVE trackers. We found that the digital twin accurately follows the movement of the real robot, enabling non-hampered task performance in a virtual environment. Furthermore, our validation method enabled us to accurately calculate clinically-relevant outcome measures from the digital twin, which may be relevant for telerehabilitation applications. This study is a preliminary effort toward exploring the potential of digital twins in neurorehabilitation for enhancing post-stroke recovery.

Acknowledgements

The authors would like to thank the VR Zone of the TU Delft New Media Centre, A. van den Berg, and A. Elferink for their support in creating the digital twin and their advice on Unity.

References

[1] J. M. Veerbeek, A. C. Langbroek-Amersfoort, E. E. H. van Wegen, C. G. M. Meskers, and G. Kwakkel, "Effects of robot-assisted therapy for the upper limb after stroke," *Neurorehabilitation and Neural Repair*, vol. 31, pp. 107–121, 2 2017.

[2] J. Mehrholz, A. Pollock, M. Pohl, J. Kugler, and B. Elsner, "Systematic review with network meta-analysis of randomized controlled trials of robotic-assisted arm training for improving activities of daily living and upper limb function after stroke," *Journal of NeuroEngineering and Rehabilitation*, vol. 17, pp. 1–14, 6 2020.

[3] V. Klamroth-Marganska, J. Blanco, K. Campen, A. Curt, V. Dietz, T. Ettlin, M. Felder, B. Fellinghauer, M. Guidali, A. Kollmar, A. Luft, T. Nef, C. Schuster-Amft, W. Stahel, and R. Riener, "Three-dimensional, task-specific robot therapy of the arm after stroke: a multicentre, parallel-group randomised trial," *The Lancet Neurology*, vol. 13, pp. 159–166, 2 2014.

[4] N. Wenk, K. A. Buetler, J. Penalver-Andres, R. M. Müri, and L. Marchal-Crespo, "Naturalistic visualization of reaching movements using head-mounted displays improves movement quality compared to conventional computer screens and proves high usability," *Journal of NeuroEngineering and Rehabilitation*, vol. 19, pp. 1–23, 12 2022.

[5] N. Wenk, J. Penalver-Andres, K. A. Buetler, T. Nef, R. M. Müri, and L. Marchal-Crespo, "Effect of immersive visualization technologies on cognitive load, motivation, usability, and embodiment," *Virtual Reality 2021*, vol. 1, pp. 1–25, 8 2021.

[6] N. Wenk, M. V. Jordi, K. A. Buetler, and L. Marchal-Crespo, "Hiding assistive robots during training in immersive vr does not affect users' motivation, presence, embodiment, performance, nor visual attention," *IEEE Transactions on Neural Systems and Rehabilitation Engineering*, vol. 30, pp. 390–399, 2022.

[7] P. P. Modi, M. S. H. Sunny, M. M. R. Khan, H. U. Ahmed, and M. H. Rahman, "Interactive iiot-based 5dof robotic arm for upper limb telerehabilitation," *IEEE Access*, vol. 10, pp. 114 919–114 928, 11 2022.

[8] F. Liu, X. Han, M. Lin, X. Wu, Q. Sun, and A. Song, "Remote upper limb exoskeleton rehabilitation training system based on virtual reality," in *2019 16th International Conference on Ubiquitous Robots (UR)*. IEEE, 6 2019, pp. 323–327.

[9] N. Rohrbach, E. Chicklis, and D. E. Levac, "What is the impact of user affect on motor learning in virtual environments after stroke? a scoping review," *Journal of NeuroEngineering and Rehabilitation*, vol. 16, p. 79, 12 2019.

[10] J. Groen and P. J. Werkhoven, "Visuomotor adaptation to virtual hand position in interactive virtual environments," *Presence*, vol. 7, no. 5, pp. 429–446, 1998.

[11] N. Toothman and M. Neff, "The impact of avatar tracking errors on user experience in vr," *26th IEEE Conference on Virtual Reality and 3D User Interfaces, VR 2019 - Proceedings*, pp. 756–766, 3 2019.

[12] T. Nef, M. Guidali, and R. Riener, "ARMin III – arm therapy exoskeleton with an ergonomic shoulder actuation," *Applied Bionics and Biomechanics*, vol. 6, no. 2, pp. 127–142, jul 2009.

[13] Özhan Özen, K. A. Buetler, and L. Marchal-Crespo, "Towards functional robotic training: motor learning of dynamic tasks is enhanced by haptic rendering but hampered by arm weight support," *Journal of NeuroEngineering and Rehabilitation*, vol. 19, pp. 1–18, 12 2022.

[14] R. Rätz, F. Conti, R. M. Müri, and L. Marchal-Crespo, "A novel clinical-driven design for robotic hand rehabilitation: Combining sensory training, effortless setup, and large range of motion in a palmar device," *Frontiers in Neurorobotics*, vol. 15, p. 748196, 12 2021.

[15] F. Just, Özhan Özen, P. Bösch, H. Bobrovsky, V. Klamroth-Marganska, R. Riener, and G. Rauter, "Exoskeleton transparency: Feed-forward compensation vs. disturbance observer," *At-Automatisierungstechnik*, vol. 66, pp. 1014–1026, 12 2018.

[16] G. Kwakkel, E. E. van Wegen, J. H. Burridge, C. J. Winstein, L. E. van Dokkum, M. A. Murphy, M. F. Levin, J. W. Krakauer, C. E. Lang, T. Keller, T. Kitago, N. Nordin, V. Pomeroy, J. M. Veerbeek, and F. van Wijck, "Standardized measurement of quality of upper limb movement after stroke: Consensus-based core recommendations from the second stroke recovery and rehabilitation roundtable," *Neurorehabilitation and Neural Repair*, vol. 33, pp. 951–958, 11 2019.

[17] E. K. Antonsson and R. W. Mann, "The frequency content of gait," *Journal of Biomechanics*, vol. 18, pp. 39–47, 1 1985.

[18] S. Balasubramanian, A. Melendez-Calderon, A. Roby-Brami, and E. Burdet, "On the analysis of movement smoothness," *Journal of NeuroEngineering and Rehabilitation*, vol. 12, pp. 1–11, 12 2015.

[19] L. Kuhlmann de Canaviri, K. Meiszl, V. Hussein, P. Abbassi, S. D. Mirraziroudsari, L. Hake, T. Potthast, F. Ratert, T. Schulten, M. Silberbach, Y. Warnecke, D. Wiswede, W. Schiprowski, D. Heß, R. Brüngel, and C. M. Friedrich, "Static and Dynamic Accuracy and Occlusion Robustness of SteamVR Tracking 2.0 in Multi-Base Station Setups," *Sensors*, vol. 23, no. 2, p. 725, jan 2023.

[20] D. C. Niehorster, L. Li, and M. Lappe, "The accuracy and precision of position and orientation tracking in the htc vive virtual reality system for scientific research," *i-Perception*, vol. 8, p. 204166951770820, 6 2017.